3211

OAR RESEARCH REVIEW

OFFICE OF AEROSPACE RESEARCH ★ UNITED STATES AIR FORCE

OAR: THE RESEARCH AGENCY OF THE UNITED STATES AIR FORCE

Volume VII Number 1 January 1968

OFFICE OF AEROSPACE RESEARCH

OAR RESEARCH REVIEW

VOLUME VII NUMBER 1 JANUARY 1968

RESEARCH-ANALYSIS PROGRAM AND METHODOLOGY	3	Maj George F. Heinrich
DETONATION BY SHOCK IN SOLID PROPELLANTS	5	Dr. Bernard T. Wolfson
CHRONOLOGY OF A NEW TECHNIQUE – DOMAIN-TIP LOGIC DEVICES REVISITED	8	Dr. Hans Zchirnt
AIRBORNE GRAVITY-MEASURING INSTRUMENTS INSTALLED ON C-130 AIRCRAFT	11	Terrestrial Sciences Laboratory, AFCRL
NARROW-BAND TV TRANSMISSIONS	13	John C. Mott-Smith
SECONDARY ELECTRON EMISSIONS PRODUCED BY GAMMA RAYS	14	Edward A. Burke
A SIGNIFICANT ADVANCE IN THE STUDY OF ION-MOLECULE REACTIONS	16	Dr. T. O. Tiernan
SOLAR-INDUCED ANTENNA VOLTAGE BREAKDOWN	18	Charles E. Ellis, Jr.
SNOWFALL PROBABILITIES CALCULATED FROM CLIMATOLOGICAL RECORDS	19	Henry Salmela
THE SOLID STATE AS A MICROWAVE GENERATOR	20	Joshua H. Rosenbloom
ERROR BOUNDS FOR THE NUMERICAL SOLUTION OF A LINEAR SYSTEM OF ORDINARY DIFFERENTIAL EQUATIONS	24	Dr. Charles Keller and Dr. Karl G. Guderley

ON THE COVER:

Brigadier General Leo A. Kiley, new Commander of OAR, is shown examining a high overload chamber vortex separator used in overload studies at the Energetics Research Laboratory, ARL.

OAR RESEARCH REVIEW is published monthly by the Office of Scientific and Technical Information (RRYC), Hq Office of Aerospace Research, USAF, 1400 Wilson Boulevard, Arlington, Va. 22209. The objective of this publication is to make a positive contribution to the exchange of information concerning Air Force conducted and sponsored research activities.

JACOB SEIDEN *Editor*

DISTRIBUTION OF THIS DOCUMENT IS UNLIMITED

For sale by the Superintendent of Documents, U.S. Government Printing Office Washington, D.C. 20402 – $2.75 per year domestic, 75 cents additional for foreign mailing, 25 cents per single copy and 15 cents per Annual Index. Back issues will not be furnished.

MAJOR GEORGE F. HEINRICH
Office of Research Analyses

research-analysis program and methodology

"Research analysis" is but one of three interrelated functional areas outlined in the mission statement of the Office of Research Analyses (ORA). The two other functional areas are "mission identification" and "systems analysis." The main inputs into each of these functional areas and the interrelationships among the three areas are shown in Figure 1.

Mission identification deals with the identification of future aerospace mission concepts. Inputs to mission-identification studies include projections of technological, political, psychological, sociological, and economic factors. Outputs from mission identification include, in addition to the identification of new mission concepts, the future general-environment context, military threats, and trends in national goals, policy and doctrine. These outputs are all valuable inputs to systems- analysis studies.

Systems analysis has enjoyed long and widespread usage and needs no explanation. It should be pointed out, however, that the systems-analysis studies conducted at ORA are concerned with systems that will not be attainable in the near future. Most of ORA's system studies are concerned with weapon systems that are at least 10 years away. By performing sensitivity analysis on the subsystems of these future weapon systems, it is possible to determine areas of research and exploratory development where great gains can be made in the effectiveness of future systems. This type of analysis then leads to the third functional area and the subject of this paper, research analysis.

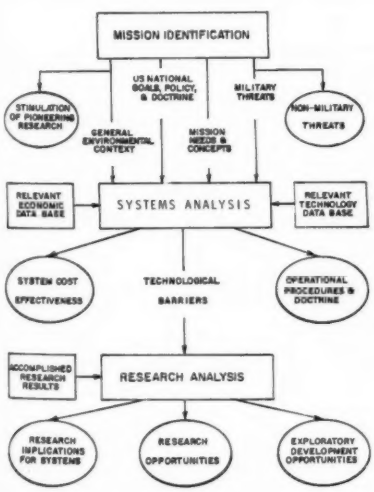

Figure 1. Relationships between ORA functional activities and end products.

This paper will describe the research-analysis program and the methodologies used for research-analysis studies. First, definitions and the objectives of research analysis will be outlined. The component parts of research analysis–technological-barrier and research-application studies–will then be described.

DEFINITIONS AND OBJECTIVES

Research analysis is defined as the determination of cost-effective applications of the results of accomplished or ongoing research and the identification of promising opportunities for mission-relevant research. The goals of research analysis are to provide the managers at two different Air Force organizations with information on which to base decisions. These two organizations include one concerned with basic-research programs–the Office of Aerospace Research (OAR) with its subordinate mission units–and another concerned with the adaptation of research results to system concepts and system developments–the Air Force Systems Command (AFSC), including its Headquarters, its Divisions, and its Laboratories. ORA assists AFSC management in exploiting research advances by the early recognition of achievable gains in technology and in systems that may result from such advances. Also, by the identification of research requirements relevant to Air Force missions, it assists OAR in determining the best allocation of research funds. This explains, in part, the close working relationship of ORA with components of both OAR and AFSC, and why ORA continues to look to both commands for guidance in its technical program.

The research-analysis program operates under two major tasks. Accomplishments of the first task, "Identification of Systems Applications of Research Results," or "research applications" for short, are addressed to system-planning agencies, primarily AFSC. Accomplishments of the second task, "Identification of Technological Deficiencies in Connection with Conceptualization and Development of Cost-Effective Aerospace Systems," or "technological barriers" for short, are addressed primarily to OAR, at least to the extent that the technological deficiencies may imply a lack of knowledge. This lack of knowledge presents an opportunity to perform mission-relevant research. However, accomplishments of the second task may also be addressed to the AFSC and other technological laboratories, depending upon the nature of the requirements envisioned for removing the technological deficiencies.

RESEARCH-APPLICATION STUDIES

A research-application study originates with an advance in a particular research area. The first step in such study, as shown in Figure 2, is to employ the results of this advance in a conceptual system to fulfill a continuing or future Air Force requirement. The conceptual system is then compared with existing or proposed

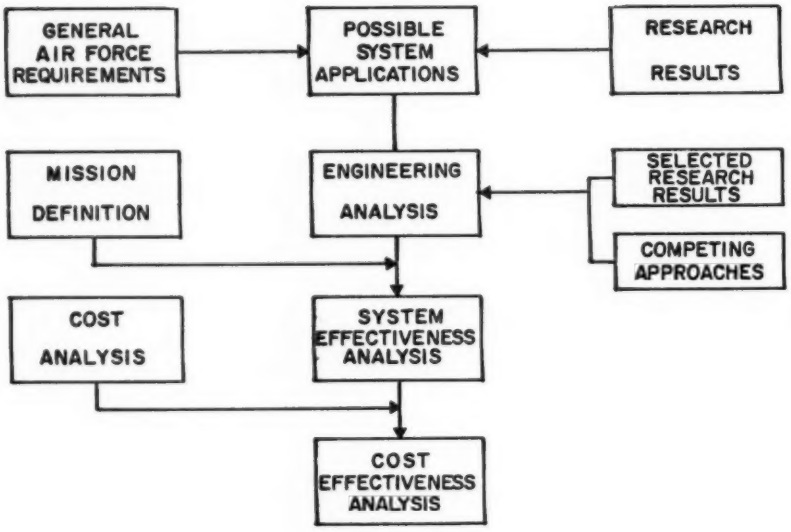

Figure 2. Research-applications methodology.

alternatives for the fulfillment of the same requirement. An engineering analysis is performed to determine the effectiveness parameters. Specific missions are proposed and the comparative systems are analyzed in terms of their effectiveness. Finally, the systems are priced and compared with the previous results to determine their cost effectiveness.

This methodology, which was developed by ORA, has now been used in two application studies, "Research-Application Study of a Magnetoplasmadynamic Jet for Space-Propulsion Application," ORA 67-0006, and "Utility of Colloid Core Nuclear Reactors for Space Propulsion," ORA 66-0001. The methodology appears to be both easy to use and effective.

TECHNOLOGICAL-BARRIER STUDIES

Technological-barrier studies normally start with a sensitivity analysis of the effects of variations of subsystem characteristics on the over-all system performance. To perform sensitivity analysis, reasonable increases in performance are postulated for the various subsystems. If the total system performance demonstrates a relatively large change with a change in a particular subsystem performance, a technological barrier is indicated.

Technological-barrier studies indicate where advances are needed to make future systems more cost effective. However, the barriers must be interpreted in terms of research opportunities for the research community. The translation of technological barriers into research opportunities follows no set patterns. One approach is to break the most sensitive subsystem down into components. Through coordination with AFSC or OAR laboratories, attempts are made to identify the weak subsystem components. Research necessary to improve component performance or to develop new, superior components is then considered to be the key to improved capability.

At ORA, two technological-barrier studies have been completed and one is in progress. The completed studies are "Technological Barriers in Boost Phase SLBM Defense," ORA 65-1, and "The Potential of an Advanced Satellite-Based ICBM Intercept System and Its Fundamental Technological Barriers," ORA 65-0005. The study currently in progress is concerned with the technological barriers limiting the cost effectiveness of a midcourse-intercept ballistic-missile defense system.

As previously mentioned, technological-barrier studies are designed to outline research opportunities for both basic-research and development agencies. In practice, the barrier studies have been more useful to the development community. This is probably because technological-barrier studies normally investigate only subsystem performance. Since basic researchers are concerned with

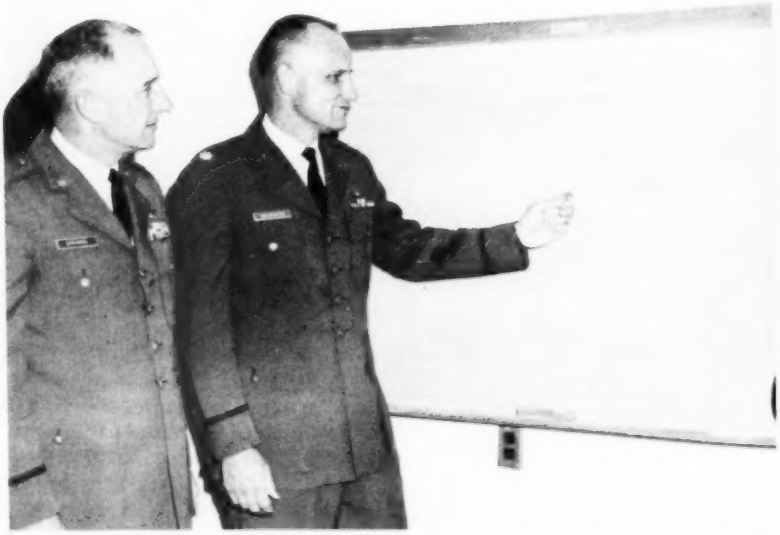

Major George F. Heinrich, right, is discussing models of interaction between the research community and technological agencies with Colonel Milton D. Sprinkel, left, Commander of ORA.

phenomena which are most closely related to subsystem components, in the future technological barriers will have to be stated in terms of subsystem components in order to be meaningful to the research community.

CONCLUSIONS

In the future ORA will continue to perform both research-application and technological-barrier studies, and will also continue to refine the methodologies used in these studies. Research-application-study methodology seems to be well in hand. However, technological-barrier-study methodology needs more refinement, particularly in the area of translating technological barriers into meaningful terms for the basic-research community. It is felt that the ORA research-analysis program has been, and will continue to be, an effective means of coupling between the basic-research community and the agencies concerned with advancements in technology.

Maj George F. Heinrich is an operations research analyst with the Office of Research Analyses (ORA). He is currently conducting research-application studies to determine effective applications of ongoing or completed research to Air Force systems. Maj Heinrich was commissioned in the Air Force after graduation from the United States Naval Academy in 1954. After taking both pilot and navigator training, he spent five years with the Strategic Air Command. He was graduated from the Air Force Institute of Technology in 1963 with an M.S. degree in Nuclear Engineering. He then served for two years with the Solid State Physics Laboratory, Aerospace Research Laboratories, after which he attended the Air Command and Staff College from 1965-1966. During this period he also completed requirements for an M.B.A. from The George Washington University. Since July 1966, Maj Heinrich has been assigned to ORA.

detonation by shock in solid propellants

DR. BERNARD T. WOLFSON
Directorate of Engineering Sciences, AFOSR

A large solid-propellant rocket motor represents a tremendous amount of energy in a metastable state. Most thermochemists, quite aware of the magnitude of this available energy, tend to worry that the well in which this particular system eventually finds itself may not be deep enough to insure peace and tranquility on the firing pad. It seems clear that solid propellants, since they yield high energies in reaction, will detonate if the diameter of the propellant is large enough and if they are submitted to a strong-enough initiating shock (a high-enough pressure, held for a long-enough time). The pertinent question is not "Will they detonate?" but rather "Under what conditions will they detonate?"

AFOSR has a continuing program of research in combustion dynamics which involves a multidisciplinary attack on fundamental problems in fluid dynamics, reactive flow, and reaction kinetics. The aspects of the program which are related to rocket safety include combustion instability, propellant sensitivity, and the relationship between deflagration and detonation.

In line with this general program, AFOSR sponsors basic research at several educational and research institutions on "initiation to detonation" in propellants and explosives. At the University of Cambridge (England), Prof. F. P. Bowden is directing an investigation into the transition from deflagration to low-velocity detonation in liquids, jels, and solids. The purpose of the Cambridge work is to obtain a better understanding of the mechanisms by which explosive waves can develop and spread in such systems.

At the Illinois Institute of Technology (IIT) Research Institute, Mrs. Hyla Napadensky is investigating the mechanism of the initiation of solid propellants by low-speed impact. The ultimate objectives of this study are to analyze the complex processes that occur during propellant deformation, to identify regions of significant energy dissipation, and to ascertain the sites of initiation in the propellant. Also, at the IIT Research Institute, Dr. T. A. Erickson will shortly be undertaking a study of the nature of sensitivity.

For several years a basic study of the detonation characteristics of low-density granular materials has been pursued under the direction of Dr. Marjorie W. Evans and Dr. Leslie B. Seely at Stanford Research Institute (SRI). Detailed experimental and analytical studies on the shock sensitivity of ammonium perchlorate (a component of many propellants and, in its own right, a low-powered, insensitive explosive) have shown a number of initiation characteristics that apparently apply to granular explosives generally and may have important implications concerning the vulnerability of propellants to shocks.

Several years ago analytic studies showed that, even for the 15-kilobar pressure required to initiate low-density granular ammonium perchlorate (AP), compressional heating is insufficient to produce a uniform temperature high enough to cause the explosive to react; the existence of hot spots had to be assumed. (1) Theoretical analysis of conductive heating of the grains by gas compressed in the interstices indicated that this was not likely to be the mechanism for producing hot spots. (2) Experimental tests of the initiation behavior of AP confirmed this calculation. The sensitivity remained unchanged, whatever the characteristics of the interstitial gas. In fact, this was the case even when the gas pressure was reduced below 10 microns. (3) Thus AP behaves much like other low-density granular explosives (4), although in view of its low power and low sensitivity one might expect it to be exceptional.

The advantage of studying initiation behavior in AP rather than in some more typical high explosive is the high-pressure threshold for shock initiation. The shocks necessary for the initiation of low-density AP, which are in the range of 15 to 25 kbars, are much easier to control and measure than the 2- or 3-kilobar shocks that are adequate for the initiation of explosives like PETN and RDX. The disadvantage of AP is that it is really not a very good explosive and shows it in its low detonation velocity. Some care must be taken to choose a suitable particle size and density so that the detonation velocity will be different enough from the velocity of the initiating shock to permit characterization of the initiation zone.

A fairly complete study of the initiation behavior of 13-μ (median-particle-size) AP has been made at density 1.0 g/cm^3 (porosity m$\simeq$2). Shocks were produced with precision high explosives and adjusted to the proper pressure with multilayered attenuator systems. The most complete was a series of 14 explosive experiments, each involving 6 to 8 determinations, all carried out at an initiating shock pressure of 24 kbars. Such a shock has a velocity of about 2.75 mm/μsec and goes over rather suddenly to a detonation velocity of 3.75 mm/μsec after a travel of about 15 mm in the AP. From the measured velocity of the shock in the AP and the measured particle velocity in the brass

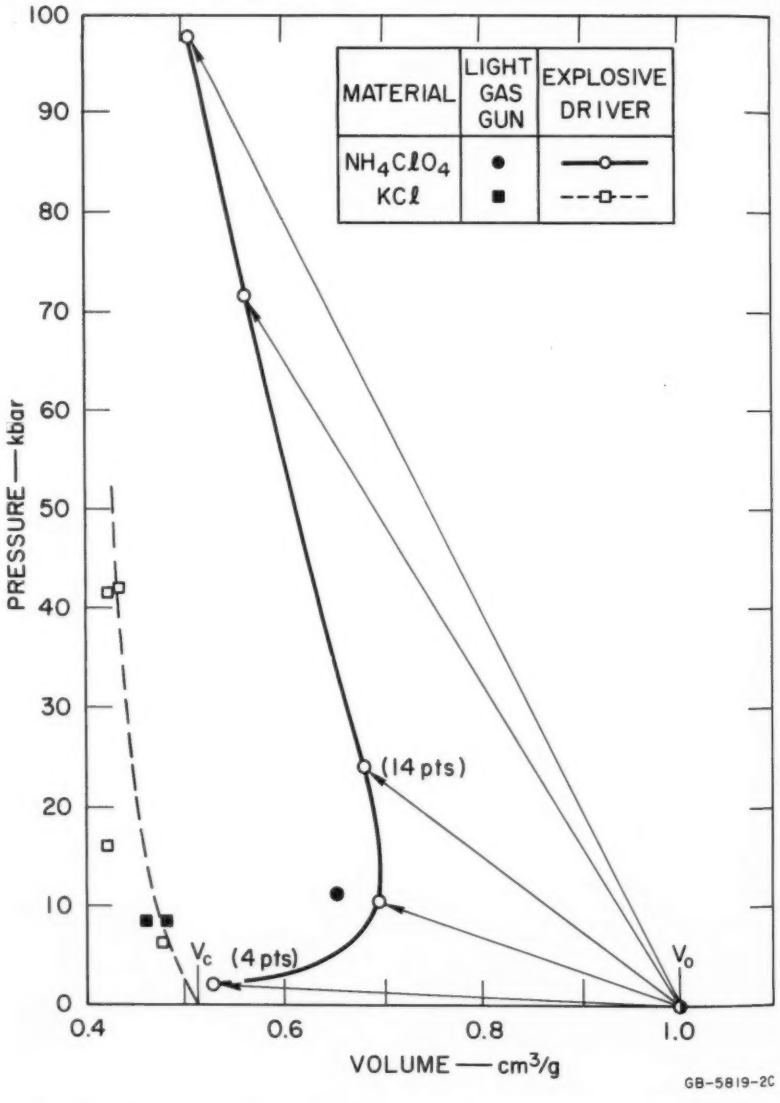

Figure 1. Shock compression curves of porous ammonium perchlorate and potassium chloride. The locus of shocked states for the NH_4ClO_4 has a positive slope for weak shocks, whereas the slope of the KCl curve is everywhere negative. The difference between the two curves in the region from 10 to 40 kilobars is ascribed to chemical reaction in the hot spots at the shock front for NH_4ClO_4, whereas the KCl is inert. Similar results have been obtained for NaCl at the same porosity (m$\simeq$2).

driver plate one can determine all the mechanical variables in the explosive.* The data are displayed in the pressure-volume plane in Figure 1. The starting condition for all the experiments was at V_o, and the shock processes at various pressures in porous AP are indicated by the arrows. Note that in the region below 10 kbar the harder you hit the AP aggregate the bigger it gets! This sort of backwards Hugoniot curve has been noticed by the Russians in inert granular material, but for porosities of 3 or greater, and never for m = 2.

When this was first discovered, the SRI team examined the possibility that it was entirely an effect of heterogeneity, but soon began to suspect, in view of the Russian results, that it was due to chemical reaction. Two lines of work were followed to make this conclusion more definite. In the first place, check experiments were run under crucial conditions by an entirely different technique using a light-gas gun instead of an explosive system to generate the shocks. These experiments confirmed the earlier results. Secondly, experiments were run on a similar granular material of such a nature that no chemical reaction could possibly occur. Potassium chloride was chosen for these comparison experiments, since the crystal has very nearly the same density as AP, and the sound velocities are also very close. Compacts of 13-μ particles at 1 g/cm^3 show sound velocities that are also very nearly the same for the 2 materials.

It is of course impossible to find an "inert AP" with every property identical to real AP except reactivity. Nevertheless, the reactive NH_4ClO_4 shows a dramatic qualitative difference from the inert KC1 that cannot be explained as a physical difference of the granules or as experimental error. The importance of this difference is that it appears in quantities derived from measurements made on the shocks before the transition to detonation. Thus, the indicated chemical reaction is in shocks as soon as they enter the AP aggregate. Initiating shocks have sometimes been considered essentially inert during this early period before initiation; but the data obtained at SRI indicate that chemical reaction starts at the time of introduction of the shock into the granular aggregate.

This brings us back again to the hot spots that are necessary to explain the shock sensitivity of explosives. These hot spots are concerned with the spaces between the grains and are produced during the collapse of the pressing. In shocks so strong that there is no precursor, hot spots occur at the very front of the wave when the aggregate is collapsed. It is not too surprising, then, that chemical reaction occurs at the front of the wave in these very hot regions. Furthermore, it seems likely that the amount of initial reaction in the hot spots is greater the larger the pressure of the entering shock. Major points remaining for investigation are the amount of subsequent reaction in the flow behind the front and the mechanism by which the full-strength wave is achieved.

Currently, work at SRI is directed toward studying the hot spots and relating their properties to the shock-to-detonation transition. It is quite easy to obtain photographs of hot spots in granular aggregates when collapsed by a strong shock. Figure 2 shows an image-converter picture of hot spots produced by a 55-kbar shock when it collapses an aggregate of 2-mm KC1 grains. The remaining problem is to demonstrate that such regions of

Figure 2. Hot spots in porous potassium chloride. The picture was taken with an image converter at an exposure time of 10^{-7} sec on Polaroid film with an ASA speed of 10,000. The shock entered an aggregate of 2-mm KC1 grains at settling density from a thoroughly blackened Plexiglas attenuator in which the pressure was about 55 kilobars. The exposure was timed to record the light just as the shock emerged from the surface of the grain bed. The interstitial gas was methane.

**The assumption of a hydrodynamically significant average pressure in a quite-heterogeneous material is a point whose significance is being examined in a number of laboratories, both here and abroad.*

high temperature continue to exist as the pressure is lowered into the range of shock strength that will cause detonation with a measurable time lag. (The lag is expected to be noticeable at about 30 kbars for grains of AP 1 mm in diameter.) An attempt will then be made to study the spectroscopic properties of the hot spots with photomultiplier-filter combinations. Such information on the size and temperature of hot spots is expected to clarify the details of the initiation process.

The SRI work, leading to a clear understanding of initiation processes in low-density granular materials, provides a firm scientific basis for the design of safe ignitors, initiators, detonators and other explosive components. What has been learned about interstitial chemical reaction has already been useful in guiding work on propellant degradation. One expects that composite propellants will be rendered ineffective by shocks that are strong enough to spall the grain surface or de-wet the constituent particles. Such mistreated propellants will then be vulnerable to interstitial chemical reaction if they experience other shock either because of explosive attack or because of combustion instabilities in the subsequent firing of the rocket.

The over-all effort on detonation sensitivity, deflagration, and the relationship between subjects is producing definite progress toward the fulfillment of Air Force research objectives in the field of combustion dynamics. We are in fact gaining the basic understanding necessary to build safe, invulnerable rocket engines and rocket components.

REFERENCES

(1) Evans, Marjorie W., C. M. Ablow, B. O. Reese, and A. B. Amster, "Shock Sensitivity of Low-Density Granular Explosives," in Proceedings of International Conference on Sensitivity and Hazards of Explosives, U. K. Ministry of Aviation, Waltham Abbey, England, Session 2, Paper No. 6, 1963.

(2) Ablow, C. M., Y. D. S. Rajapakse and Marjorie W. Evans, "An Analysis of the Shock Initiation of Granular Explosives by the Gas Compression-Conduction Mechanism," in Preprints of Meeting of Western States Section of the Combustion Institute, Santa Barbara, California, 26 October 1965.

(3) Evans, Marjorie W., B. O. Reese, and L. B. Seely, "Shock Initiation of Low-Density Pressings of Ammonium Perchlorate," in Fourth Symposium on Detonation, U.S. Government Printing Office, ACR 126, 1966, pp. 359-372.

(4) Seay, G. E. and L. B. Seely, "Initiation of a Low-Density PETN Pressing by a Plane Shock Wave," Journal of Applied Physics, 32, 1092-1097, 1961.

CHRONOLOGY OF A NEW TECHNIQUE...DOMAIN-TIP LOGIC DEVICES REVISITED

DR. HANS ZCHIRNT, Data Sciences Laboratory, AFCRL

Occasionally it is entertaining and even instructive to reconstruct the history of a successful new development. It often happens that the result is far removed from the original interest–that the promising goal that motivated the start of an original research project proved unattainable and that the very obstacles encountered in its pursuit were found to contain hidden virtues that led to success in a different direction. The history of the recently developed domain-tip logic devices is a case in point. Here is the story.

Around 1959, Dr. Harrison Fuller, of the Laboratory for Electronics in Boston, approached the Air Force Cambridge Research Laboratories with a proposal for the development of a high-density magnetic thin-film storage device. The proposal was accepted and pursued under AFCRL sponsorship.

In conventional digital storage on magnetic tapes or drums, small magnetized areas are created in the recording medium by the write head (Figure 1). On playback, these areas are sensed by the reading head. What the reading head senses is actually the stray fields emanating from the boundaries–the domain walls–between areas of opposed magnetization. No signal is generated while the head traverses the uniformly magnetized regions themselves. The spacing between domain walls and, thereby, the storage density are determined by the geometry of the read/write heads, which have to have a gap of substantial width compared to the thickness of the domain walls. (As a result, the digit density on a digital magnetic tape was limited, at the time of the submission of the proposal, to about 200 bits per inch. On modern equipment, densities up to 800 bits per inch are used.)

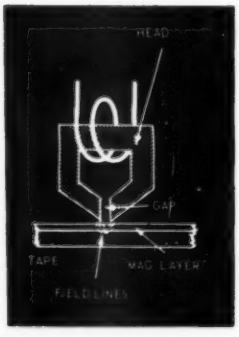

Figure 1. Write head creates small magnetized areas in recording medium.

Dr. Fuller proposed the following scheme for a high-density magnetic thin-film memory: information is stored, similarly to tape storage, in a magnetic film of relatively high coercivity with the domain walls packed as closely as possible. (It was hoped that a very high density would be feasible due to the microscopic thickness of the walls.) For readout, a second thin film of less coercive material is placed very close to the storage film. An inhomogeneous magnetic field is now

applied to the film sandwich in such a manner that its highest value is at the, say, left end of the film and its magnitude decreases linearly towards the right. As the amplitude of this field is increased, a single domain wall (Figure 2) is formed at the left end and begins to travel towards the right at an essentially uniform velocity, except that it is temporarily accelerated or retarded as it traverses the stray fields of the domain walls recorded in the storage film. These changes in propagation speed are sensed by a pickup coil wrapped around the entire structure and provide a serial nondestructive readout of the stored information.

This scheme, with its elegant avoidance of moving parts subject to wear and with its promise of high storage density and reasonable speed, seemed to be an answer to many wishes. As work progressed, however, some fundamental difficulties appeared which considerably spoiled the beauty of the original concept. One, of less concern for this story, was that accurate placement of domain walls in the storage film proved difficult. This reduced storage density significantly below expectations. The other serious problem was that great difficulties were encountered in producing the required uniform, reproducible motion of a single straight domain wall across the readout film. This was particularly true when rapid motion was attempted to obtain a high-output bit rate. The reason for this was found to be quite fundamental. It involves the simultaneous presence of two different mechanisms of magnetic polarity reversal. At low applied switching fields, causing slow reversal of magnetization, a domain of reversed magnetism grows by motion of its walls perpendicular to the wall (Figure 3), thus expanding the domain until the entire film is magnetized in the direction of the applied field. As the switching speed is increased by increasing the driving field, spike-shaped regions of reversed magnetism form which grow in the direction of the tip of the spike (Figure 4)–hence the name "domain-tip propagation." Since this creates partially switched regions in the film ahead of the desired domain wall, current readout is impossible. Hence, the hope of

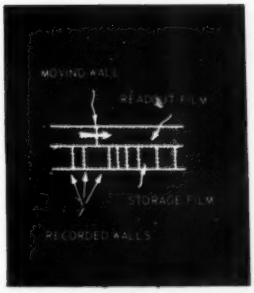

Figure 2. As amplitude of inhomogeneous magnetic field applied to film sandwich is increased, single moving domain wall is formed on readout film.

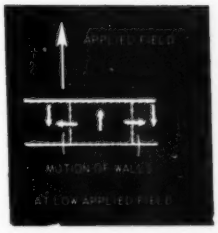

Figure 3. At low applied switching speeds, causing slow reversal of magnetization, a domain of reversed magnetism grows by motion of its walls perpendicular to original domain wall.

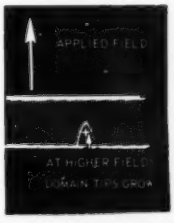

Figure 4. As increasing driving field increases switching speed, spike-shaped regions of reversed magnetism form and grow in direction of tip of spike.

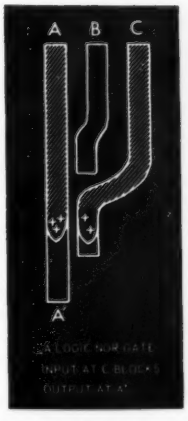

Figure 5. Logic "NOR" gate. Input at C blocks output at A'.

having a high-density, reasonably fast memory had to be abandoned.

On the other hand, the rather long, narrow domains resulting from domain-tip propagation have some attractive properties. First, domain tips propagate rather rapidly with a speed on the order of 5.10^5 cm/s, as opposed to domain walls at about 10^4 cm/s. Second, if the applied field is at an angle to the easy axis of magnetization of the film, the tip will also propagate at a similar angle. Third, interaction between domain tips is much stronger than interaction between single domain walls. This is because domain tips, due to their elongated shape, behave like bar magnets with the magnetic "charges" separated by a substantial distance, while domain walls, with their closely spaced opposite charges, have stray fields that decay rapidly with increasing distance.

Attempts to exploit these properties for logic devices proved successful. Their operation has been described in earlier literature. To recapitulate quickly, a simple logic gate is shown in Figure 5. The channels seen are strips of low coercivity obtained by removing the aluminum coating from the glass substrates on which the magnetic film is deposited. Changes of magnetization occur in the channels only and not in the remainder of the film, which is of higher coercivity. Thus, the channels serve as guides for the propagating domain tips. The width of the channels controls, to a degree, the speed of the domain-tip propagation. The sketch shows a logical "NOR" gate. A domain tip nucleated at A will propagate down towards A' when an external field is applied. It will reach A' only if neither B nor C contain domain tips. Otherwise, since like poles repel each other, it will be blocked and no output will appear at A'. The structure, therefore, performs the logic "NOR" function, which is sufficient to synthesize all combinatorial logic functions.

Recent progress is shown in Figure 6, which illustrates an eight-digit adder/subtractor. It shows the input registers (top), the summing/subtracting network (the spidery structure in the center), and the readout and output storage registers together with the conductor pattern providing

the driving fields. Various devices of this and related kinds have been operated satisfactorily.

While research on domain-tip logic is continuing, a number of practical applications have been implemented. A domain-tip propagation logic (DTPL) shift register is available as a commercial product. A DTPL counter is under consideration as a timer for fuze applications. A push-down list memory and a first-in first-out communications buffer memory is nearing completion with sponsorship by the U.S. Army. The arithmetic unit shown is another operational product, and an associative processor combining logic and memory is being worked on. All of these devices, and more and better ones to come, share the outstanding advantages of the DTPL technique: insensitivity to shock and vibration, high radiation resistance, nonvolatility of stored information, simplicity of manufacture, and small size. This combination of advantages should make these devices highly useful in a large variety of military and commercial applications.

Such is the history of a research project that started out in one direction, seemed to fail, and became a success in a different way. This reminds one of a man named Böttcher,* in the Electorate of Saxony, who set out to make gold for Augustus I, the Elector of Saxony and King of Poland. Augustus was an eager contract monitor since he was a man of expensive tastes. Mr. Böttcher never succeeded in making any gold (except possibly his cost-plus); but his failure gave us Meissen porcelain, the first true hard porcelain to be made in Europe. This serendipitous discovery proved to be a "gold mine" for Augustus.

**Johann F. Böttcher (Böttger), 1682-1719.*

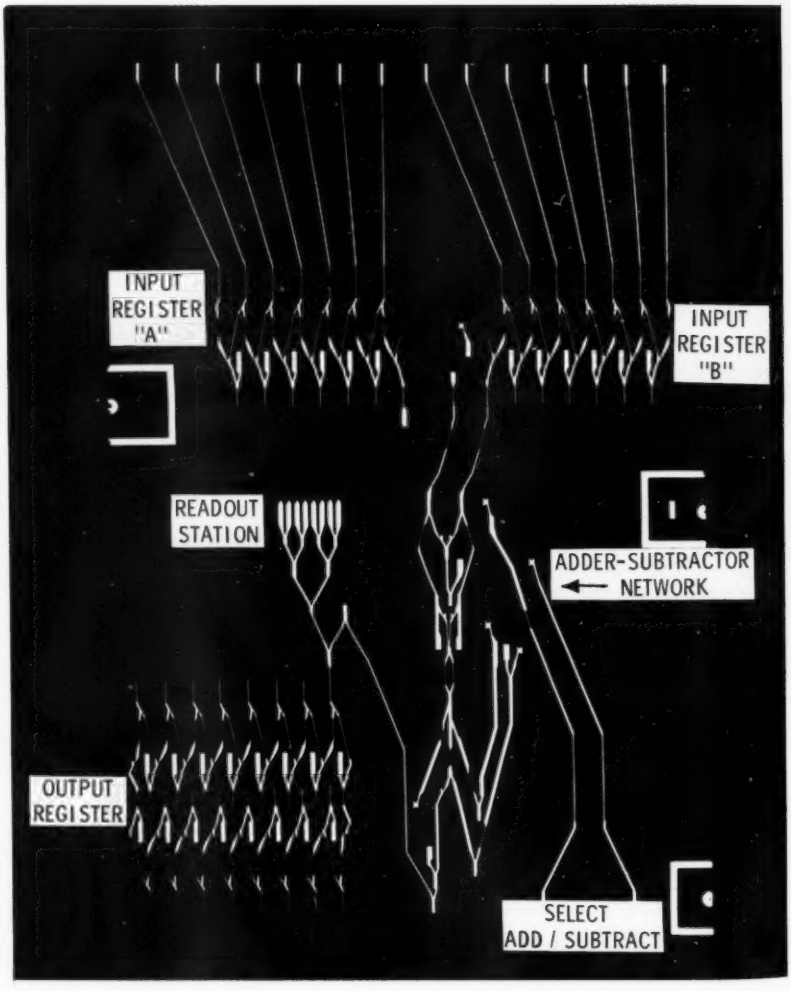

Figure 6. DTPL arithmetic unit, partial view. Complete unit consists of two of these films sandwiched together in registration with each other and with driving and sensing printed circuitry.

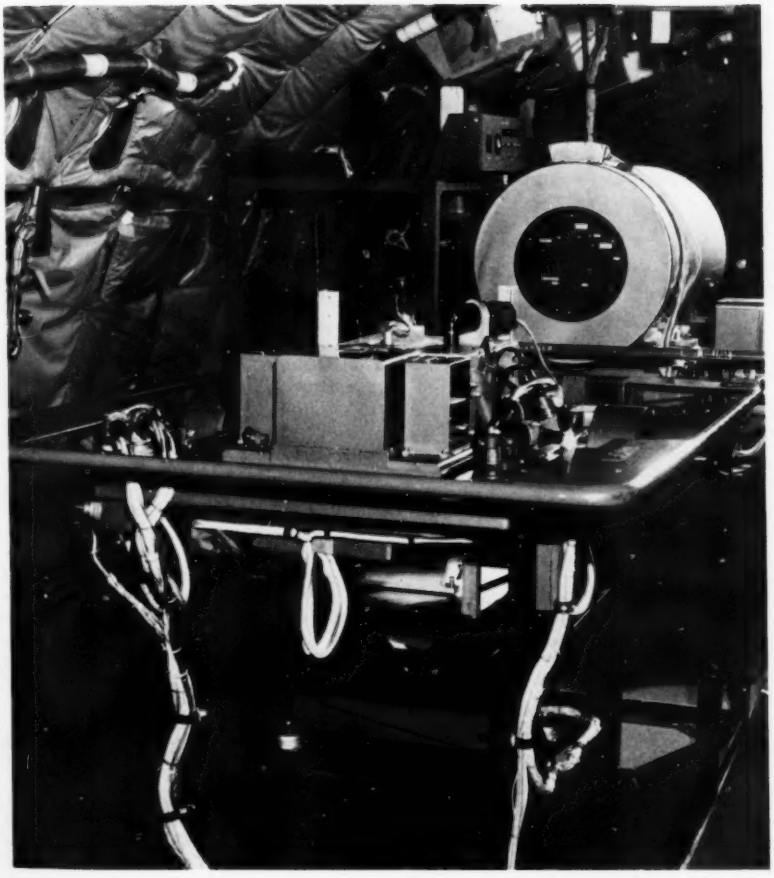

airborne gravity-measuring instruments installed on C-130 aircraft

TERRESTRIAL SCIENCES LABORATORY, AFCRL

Extremely sensitive airborne gravity-measuring instruments have recently been installed by the Air Force Cambridge Research Laboratories, OAR, on a C-130 aircraft. The newly instrumented aircraft left AFCRL's home base at L. G. Hanscom Field, Mass. on October 20, 1967 for a series of flight tests which, over a period of several months, was to take it over much of the continental U.S. These currently modified prototype instruments will be evaluated against the known gravity values of three different gravity test ranges in the United States.

From Ellsworth AFB, South Dakota, during the period from October 20 to December 23, 1967, the C-130 surveyed the North Range, covering the states of Washington, Oregon, Montana and South Dakota. For the remainder of the program, with Forbes AFB, Topeka, Kansas as the staging base at the outset, the C-130 will survey the South Range and the Gulf of Mexico Range during the period from January 9 to April 1, 1968. The South Range includes Colorado, Texas, Kansas and Oklahoma; the Gulf of Mexico Range takes in the Gulf-Coast offshore areas of Texas, Louisiana, Mississippi, Alabama and Florida. Airborne measurements are particularly effective for surveys over

oceans and inaccessible land areas.

AFCRL has greatly improved airborne gravity instrumentation survey techniques and data-reduction programs since beginning the program in 1958. Three airborne gravimeters are installed on the C-130. They are a LaCoste-Romberg, an Askania-Graf, and a Pendulus Integrating Gyro Accelerometer (PIGA). Associated with the PIGA meter is an AJN-10 Inertial Reference Unit. All of these instruments are mounted on highly stabilized platforms.

The instrumentation complex also includes the following: an airborne profile - recording unit for providing a record of vertical aircraft ground clearances and relative deviation from planned flight level; a Doppler radar; a navigational computer; an Astrotracker for navigation; and a T-11 camera system for identifying landmarks along the flight paths.

The program calls for more than 350 hours of flying time and about 60 flights. Project scientist is Bela Szabo of AFCRL. Members of AFCRL's Terrestrial Sciences Laboratory aboard the aircraft during the tests are Robert M. Perry, flight director, and Lt. Colonel Ogden C. Eggleston, assistant flight director.

Lt Col Ogden C. Eggleston is a geodetic research officer with the Gravity Branch, Terrestrial Sciences Laboratory, AFCRL. He is presently engaged in the navigational aspects of airborne gravity research and airborne gravity data reduction. Col Eggleston attended Drake University, the University of Houston, and the University of Omaha, and was graduated from the Ohio State University in 1965 with a B.S. in Geodetic Science. After Army service from 1940 to 1943, he was commissioned as a navigator in the USAF and served until 1945. Recalled to active duty with the Air Force as a navigator in 1951, he remained in that field until his transfer to the Air Force Institute of Technology in 1963.

Mr. Robert M. Perry, a geodesist with the Gravity Branch, Terrestrial Sciences Laboratory, AFCRL, is currently engaged in flight-testing airborne gravity-meter systems. Since joining AFCRL in 1959, his work has been concerned with the airborne gravity-meter program, worldwide gravity nets, and the development of new and improved gravity-sensing instrumentation. Mr. Perry attended Colby College in Waterville, Maine, and Northeastern University in Boston, Mass. During World War II, he served with the Coast Guard in the Atlantic Sea Frontier. Before coming to AFCRL, he worked as a cartographic and surveying engineer with the Geological Survey, and as a supervisory cartographer with the Army Map Service.

JOHN C. MOTT-SMITH
Data Sciences Laboratory
AFCRL

narrow-band TV transmissions

TV-picture transmission with a 5-to-1 reduction in the bandwidth normally needed to transmit TV pictures has been demonstrated at AFCRL. Black-and-white TV pictures with no apparent picture degradation can be transmitted over a 160-kHz channel compared with a normal bandwidth of 4 MHz used for commercial television. This technique takes advantage of integrative properties of the human visual system.

The slower transmission rate is achieved by pointwriting the picture. Pointwriting contrasts with the familiar line scan used in normal picture transmission and reconstruction. The points of light which make up the final picture are presented at different areas on the screen in a pseudorandom manner. Bandwidth reduction can be accomplished with no picture degradation provided the bandwidth reduction factor does not exceed about 5.

Picture quality ultimately involves subjective definition. Therefore, tests of the AFCRL technique take place in a viewing room in which test subjects give subjective evaluations of picture quality. Here various types of scans are generated under conditions of controlled brightness, contrast, resolution and frame rate. Flicker fusion, motion resolution, effects of phosphor persistence, gray-level fusion and figure detection in pictures of drastically reduced pointwriting rate are evaluated.

In one picture-evaluation experiment, a uniform field containing a moving dark rectangle is presented. Frame periods (the time taken to write all points in the picture raster) were varied from 1/60 second to 6 seconds. If the contrast between the rectangle and the background is low, a fairly high point rate is required for perception. As the contrast is increased, the rate may be decreased to achieve the same perception probability. In the extreme of black or white, the rectangle can still be perceived even when 6 seconds are needed to pointwrite the entire picture, although the viewer is exposed to the partly completed picture for only 1 second. Thus, the

Mr. Mott-Smith examines oscilloscope display of data just processed by computer.

subject discerns the picture even though more than 80 percent of the pseudorandomly generated points that make up the total picture are not seen at all.

The AFCRL pointwriting TV system is breadboarded from standard off-the-shelf components. Now under study is the optimum phosphor persistence time for low frame-rate television using a variable-memory storage tube to simulate the phosphor. It is anticipated that decay times around 1/10 second will be desirable, a value very difficult to achieve with current phosphors.

It is unlikely that a TV transmission system based on the pseudorandom pointwriting technique would have application in normal TV transmission. A potential commercial use, however, does exist in videotelephone applications. Because of the relatively smaller amounts of power needed to transmit a narrow-band picture, it could prove valuable in the transmission of TV pictures from satellites or from deep space–or in any situation where power is limited or where bandwidth is a critical factor.

Mr. John C. Mott-Smith is a supervisory research general physical scientist with the Synthetic Coding Branch, Data Sciences Laboratory, AFCRL. His current work involves the processing of visual information, bandwidth and power-reduction techniques for image transmission, and pattern recognition in visual systems. He received his B.S. (1952) and M.S. (1953), both in Physics and both from the Massachusetts Institute of Technology. Mr. Mott-Smith entered the Air Force from ROTC in 1952. In 1953, he was assigned to the Propagation Laboratory of the Air Force Cambridge Research Center, AFCRL's predecessor, where he applied statistical techniques to propagation studies, radiometry, and atmospheric absorption, and also studied the theoretical problems of communication and antijamming. After leaving the service in 1956, he returned to AFCRC to study Air Force communications problems. Mr. Mott-Smith is a member of the Institute of Electrical and Electronics Engineers and the American Association for the Advancement of Science.

SECONDARY ELECTRON EMISSIONS PRODUCED BY GAMMA RAYS

EDWARD A. BURKE
Solid State Sciences Laboratory, AFCRL

A new 22,000-curie cobalt-60 source of gamma rays was delivered to AFCRL in October 1967. The new source will replace the previous cobalt-60 source that had decayed from 7,200 to about 3,200 curies over the past 6 years. This new source, plus a new source configuration, will provide a much higher flux of gamma rays at the target area.

Over the past year, AFCRL has studied secondary electron emission from solids bombarded with gamma rays. The emission of secondary electrons can cause disruptive transient effects in electronic systems. When this happens, the missile or vehicle under the control and guidance of these electronic systems may fail in its mission. The magnitude of transient effects from secondary electron emission induced by gamma rays has been uncertain due to an almost total lack of experimental data or suitable theory.

Secondary electron emission can be produced by electron bombardment as well as by gamma rays. Quite

a bit of data on secondary electron emission produced by low-energy electron bombardment exists in the literature. But data are lacking for emission produced by high-energy electrons or by gamma rays. The AFCRL experiments were designed to determine whether the data and associated models of secondary emission from low-energy electron bombardment are applicable to gamma-ray and high-energy-electron-induced electron emission. AFCRL determined that, in general, they are.

In the AFCRL experiments, measurements were made of the secondary electron yields from a number of metals–silver, gold, aluminum, platinum, and so on–subject to cobalt-60 gamma rays. Calculations were made on the basis of emission yield per unit of deposited energy. This analytical approach affords the advantages of mathematical simplicity over measurements of yield per incident photon. The experimental configuration employed was that of a multiple parallel plate chamber.

Prior to the experiments, the AFCRL researchers predicted that their gamma-ray results would be within 30 percent of those indicated by electron-bombardment models. The results were actually much better. The values predicted for silver, platinum, and gold were within 10 percent of the measured values. (The values are expressed in terms of emission efficiency, or amps/cm^2 for 1 rad/sec x 10^{-13}.) Of the metals measured, the largest discrepancy was in the aluminum measurements, where the secondary electron emission was 60 percent greater than predicted. This was explained by the presence of an oxide layer on the aluminum which is known to have a strong influence on electron emissions.

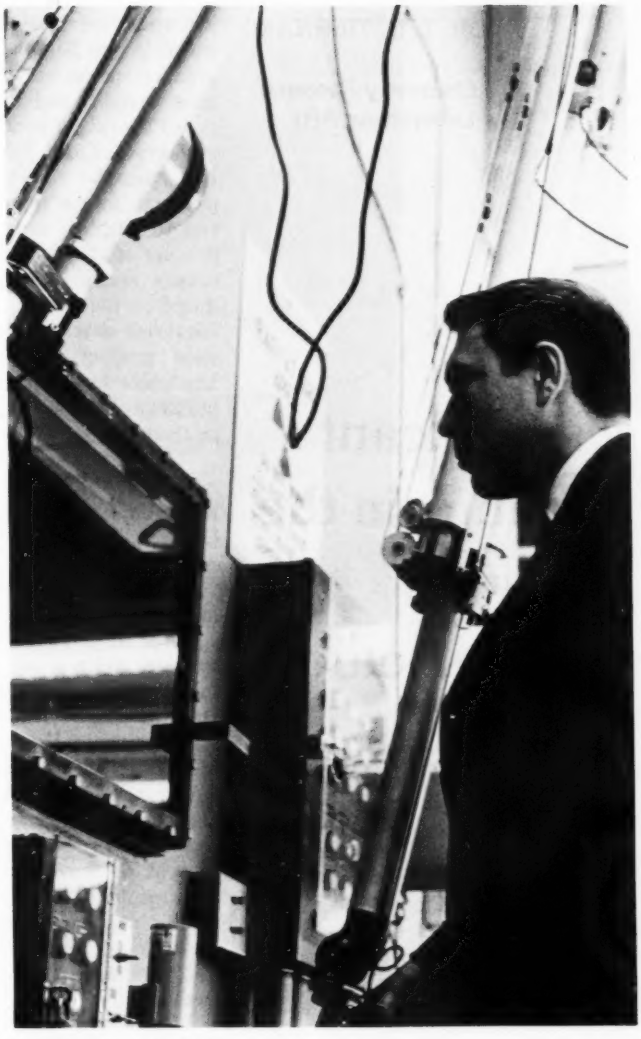

Mr. Burke exposes samples in cobalt-60 hot cell for secondary-emission experiment.

Mr. Edward A. Burke, a research chemist with the Radiation Effects Branch, Solid State Sciences Laboratory, AFCRL, is studying the low-temperature electron bombardment of solids, and making experimental determinations of secondary electron emission for application to irradiated electronic devices and circuits. He has a B.S. in Chemical Engineering from Northeastern University (1950), has done graduate work in organic chemistry at the Ohio State University, and has taken AEC-sponsored graduate training in radiological physics at the University of Rochester. With AFCRL since 1957, Mr. Burke has been engaged in research in radiation effects and radiation dosimetry. His work has resulted in methods for predicting charge emission from irradiated solids, a revision in atomic cascade models used in radiation-damage calculations, determinations of threshold energies for atomic displacement, and new methods for measuring low-energy X-ray and neutron spectra. Mr. Burke is a member of the American Physical Society, the Health Physics Society, and the Research Society of America.

DR. T. O. TIERNAN

Chemistry Research Laboratory, ARL

a significant advance in the study of ion-molecule reactions

Reactions between ions and neutral molecules constitute one of the most important reaction types which have been subjected to detailed examination in recent years. Because of the large reaction rates characteristic of these processes, they may be expected to play an important role in virtually any system in which ions are produced. Typical of such systems are electric discharges, plasmas, and radiation or other high-energy environments.

Ions are most conveniently studied in a mass spectrometer. In such an instrument, a beam of electrons is commonly used to produce ions which are then analyzed according to their mass-to-charge ratios. If the pressure in the ion chamber or source is increased to the extent that a small number of the ions initially produced (designated "primary" ions) undergo reactive collisions with neutral molecules, then ion-molecule reactions occur and the ionic products from these reactions are analyzed along with the unreacted primary species. Using this technique, which was employed in almost all early research in this field, both reactant and product species are produced in the same chamber and the spectrum obtained consists of peaks attributable to both types of ions. Various procedures must then be employed to assign a given ion to the appropriate category and to establish the correct reactant-product relationship. Since there are usually several "primary" ions produced in the source, and since more than one reactant often yields the same product ion, it is frequently impossible to determine uniquely the precursor of a given product by this method.

A much more sophisticated apparatus for the study of ion-neutral interactions is now being utilized by Dr. T. O. Tiernan and his colleagues at ARL. This instrument, which was developed at ARL is, in effect, a tandem mass spectrometer. (See Figure 1) It consists of a first-stage mass spectrometer which serves as an ion source for a collision chamber to which is attached a second mass spectrometer for analysis of products. Thus it is possible to select in the first stage an ion of known mass and energy, and impact it upon the neutral species of choice in the collision chamber. Analysis of the products in the second-stage spectrometer then permits one to specify unambiguously the reactions of the ion in question without resorting to additional identification methods.

One example of the usefulness of this capability is provided by a recently accomplished study of the reactions between argon and hydrogen. Here, the deuterated species, HD, was employed in order to obtain an estimate of the magnitude of isotope effects. It is clear that a single source experiment would not enable one to distinguish the products arising from the two possible reactions,

$$Ar^+ + HD \rightarrow (ArH^+, ArD^+) + (D, H) \quad (1)$$

$$HD^+ + Ar \rightarrow (ArH^+, ArD^+) + (D, H) \quad (2)$$

since the reactions of Ar^+ and HD^+ could not be examined individually. However, the tandem data presented in Figure 2 show that both reactions do occur, but that isotope effects are rather different in the two cases. This may be related to differences in vibrational energy for the two ionic reactants.

A further significant feature of design of the tandem mass spectrometer is the capability for operation at very-low-impacting ion energy. Beams of experimentally useful intensity may be obtained over the energy range 0.2 - 100 eV with an energy spread of only 0.3 eV. Since many of the environments in which ion-molecule reactions occur involve ions at near-thermal energies, the low-energy capability of this instrument permits a close analogy between reactions observed by this mass-spectrometric technique and those actually occurring, for instance, in the upper atmosphere or in discharges. Also, the possibility of obtaining vir-

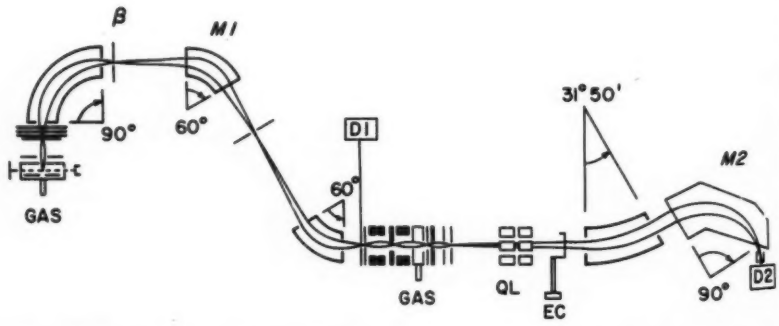

Figure 1. Schematic of tandem mass spectrometers. β is energy-resolving slit and M1 is magnet of ion gun spectrometer. D1 is ion detector-monitor for ion gun. QL is quadrupole lens, EC is movable electrometer for total ion-current measurement, M2 is mass analyzer, and D2 is final detector for product ion analyzer.

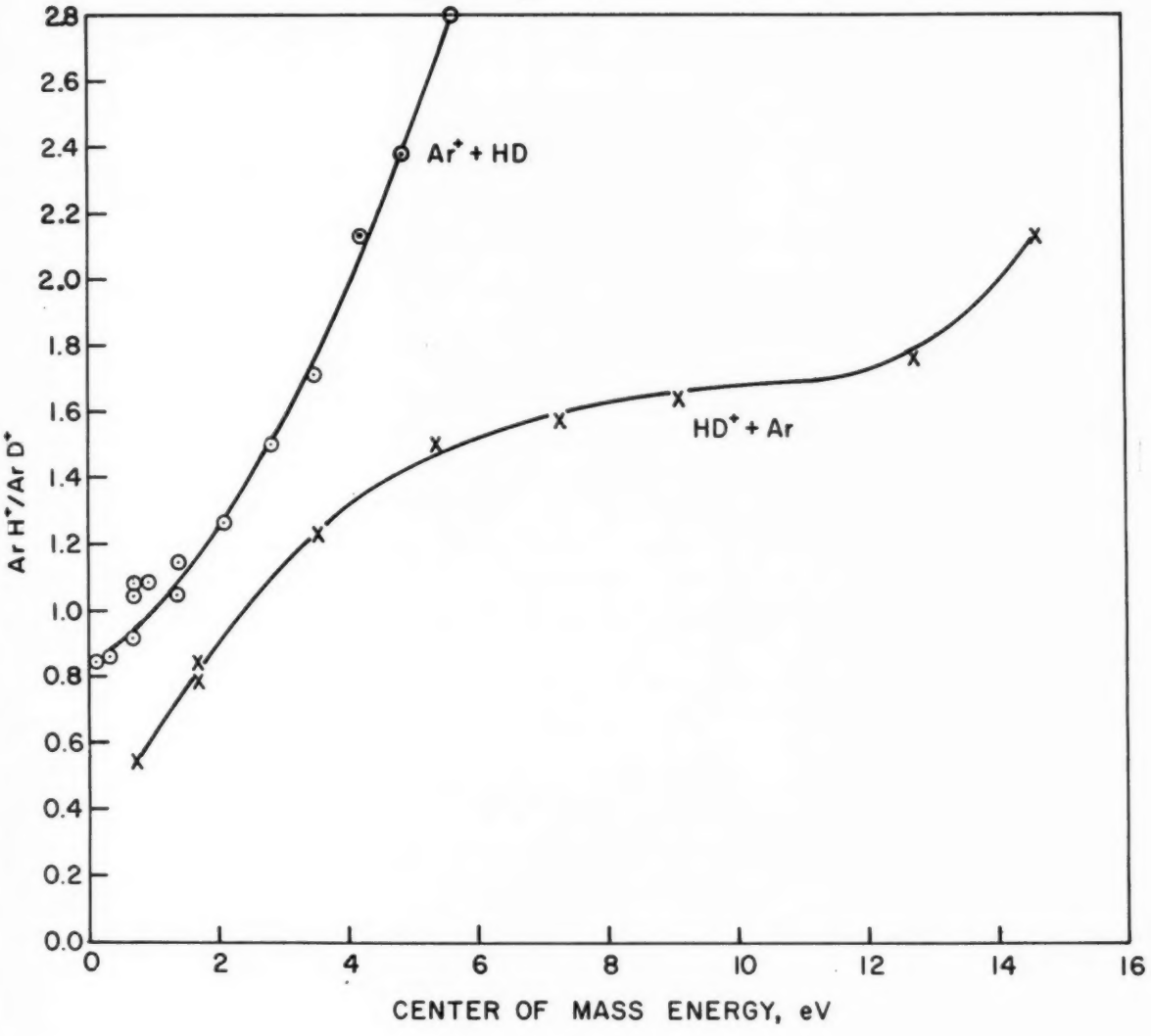

Figure 2. Isotope effect for ion-molecule reactions in HD-Ar system as function of kinetic energy in center of mass.

tually monoenergetic ion beams provides a means of readily testing the energy dependence predicted by currently existing theories of ion-neutral interactions.

With the recognition that ion-molecule processes are significantly involved in determining the chemical changes which result from the interaction of radiation with matter, fundamental studies of these reactions have become a requirement for logical planning and design. Information derived from such studies should have wide application to such problems as the radiation degradation of materials, the biological effects of nuclear emissions, and knowledge of the space environment. The ARL tandem mass spectrometer is making substantial contributions to the in-depth study of this important class of reactions.

REFERENCES

(1) Futrell, J. H. and D. C. Miller, "Tandem Mass Spectrometer for Study of Ion-Molecule Reactions," Rev. Sci. Instr., 37, 1521, 1966.

(2) Tiernan, T. O. and J. H. Futrell, "Ionic Polymerization of Unsaturated Hydrocarbons," Proceedings of the 15th Annual Conference on Mass Spectrometry and Allied Topics, Denver, Colorado, May 14-19, 1967.

(3) Futrell, J. H. and T. O. Tiernan, "Ionic Reactions of Unsaturated Hydrocarbons. I. Polymerization of Acetylene," J. Phys. Chem., in press.

(4) Tiernan, T. O. and J. H. Futrell, "Ion-Molecule Reactions in Ethylene," presented at 15th Annual Meeting of the Radiation Research Society, San Juan, Puerto Rico, May 7-11, 1967; J. Phys. Chem., submitted for publication.

(5) Abramson, F. P. and J. H. Futrell, "Mass-Spectrometric Investigation of H and H_2 Transfer Reactions of Hydrocarbon Ions," J. Phys. Chem., 71, 1233, 1967.

CHARLES E. ELLIS, JR., Microwave Physics Laboratory, AFCRL

SOLAR-INDUCED ANTENNA VOLTAGE BREAKDOWN

The sun greatly accelerates the voltage breakdown of antennas carried aboard rockets and missiles. This relationship between solar light and antenna voltage breakdown was clearly demonstrated in a rocket experiment conducted by AFCRL on October 2, 1967 from Wallops Island, Virginia.

Telemetered data from a Nike-Cajun rocket showed that radio-frequency breakdown of an x-band (9380 MHz) narrow-slot antenna occurred repeatedly when the antenna was illuminated by the sun. When the antenna on the rotating nose cone turned away from the sun, no breakdown occurred. This is the first time that this solar-induced effect has been measured, although previous AFCRL experiments had suggested that sunlight could augment antenna voltage breakdown.

The October 2nd launch was designed to observe antenna voltage breakdown as a function of altitude and atmospheric density. The effects of solar illumination on antenna breakdown were a secondary feature of the experiment. To determine these effects, the payload included a photoelectric sensor. The sensor was used to indicate when the antenna was illuminated by the sun, and to provide a means for determining the spin rate of the nose cone. The antenna was powered by a 9-kw pulsed source with a 100-pps repetition rate.

Antenna voltage breakdown is essentially a coronal discharge phenomenon. An antenna that can handle high peak powers at sea level without difficulty will experience voltage breakdown at higher altitudes (above about 50,000 feet) when the insulating effect of the atmosphere is decreased. For this reason, the problem is most acute on antennas carried aboard rockets and missiles. When it occurs, there is a sudden decrease in the signal strength at remote receivers and a change in the received pulse shape.

Solar light apparently induces antenna voltage breakdown by photoionization. Where a high electric field exists, as in the case of an antenna radiating at high power, a single electron freed by photon collision can produce an avalanche in such a field. This is because each ionization event releases an additional electron which can then produce further ionization. The creation of an ionized path by this process results in antenna voltage breakdown.

Mr. Charles E. Ellis, Jr., is a research electronics engineer with the Plasma Electromagnetics Branch, Microwave Physics Laboratory, AFCRL. He is currently working on special radar systems and on the problem of voltage breakdown of antennas at high altitudes. After receiving his B.S. in Chemical Engineering from the Massachusetts Institute of Technology in 1934, he became associated with Sylvania Electric Products, Inc., where he specialized in the annealing of glass. Following service with the Air Force from 1942 to 1948, Mr. Ellis became an electronics engineer with the Wright Air Development Center, where he worked with airborne antennas. He has been with AFCRL since 1955. Mr. Ellis is a member of the Institute of Electrical and Electronics Engineers.

Using Smith chart, Mr. Ellis calculates antenna impedances.

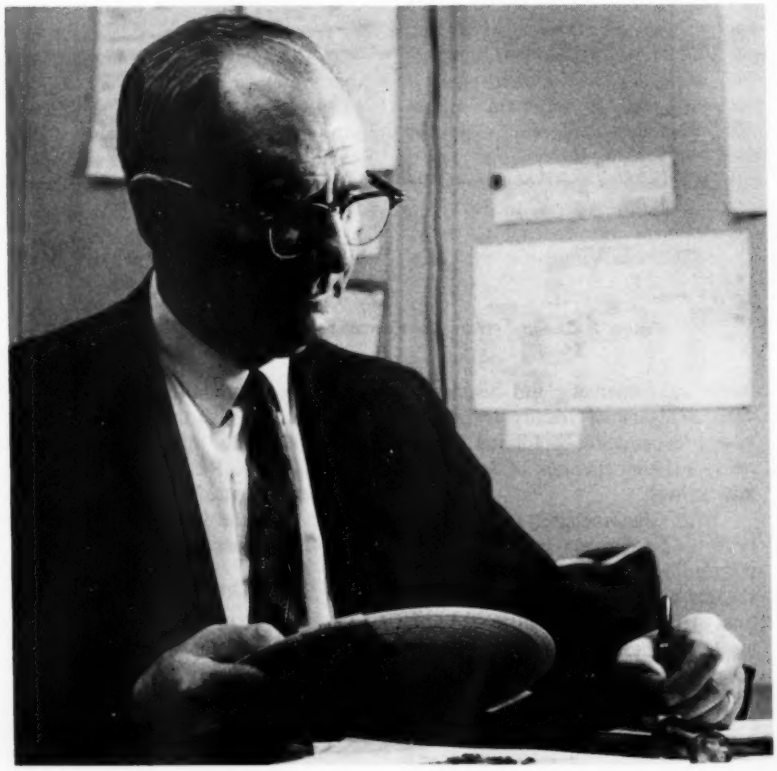

Snowfall Probabilities Calculated from Climatological Records

HENRY SALMELA, Aerospace Instrumentation Laboratory, AFCRL

Climatologists can provide the odds-maker with a pretty reliable set of probabilities on just what kind of weather the 1967-1968 winter will bring to a particular geographical area. These probabilities cannot be used to predict whether the winter will be severe or benign, but they can be used, for example, to tell the skier who likes to plan his vacation well in advance the chances of finding snow on a particular week end.

AFCRL climatologists have completed a study on snowfall in the Boston area. In this study they correlated data on snowfalls occuring from November through April of each year as far back as 1891 to determine the possibilities of snowfall in any of the winter months. During the entire 75-year period studied, 254 snowfalls occurred in January. February, with 230 snowfalls, had the second highest number. However, a greater number of snowfalls of 6 inches or more occurred in February. The earliest severe snowstorm occurred in 1940 when a furious ice and snow storm struck on Thanksgiving Day.

In Boston, measurable snowfall (0.1 inch or more) occurs on 35 to 40 winter days. Of these days, about 15 will have snowfalls of one inch or more, and about 4 will have snowfalls of 6 inches or more. Total seasonal snowfall usually averages about 60 inches. The record total annual snowfall was set during the winter of 1947-1948 when Blue Hills registered 136 inches and Logan marked 89 inches. In late January of that winter, Blue Hills, Wellesley and Newton had 42 inches of snow on the ground.

There is 1 chance in 20 that the maximum snowfall this winter in Boston will be less than 4 inches or more than 21 inches. A similar 1-in-20 chance exists that the maximum snowfall in the next 10 years will not exceed 26 inches, or that the greatest snowfall in the next 50 years will not exceed 31 inches.

From these snowfall records, it is possible to derive probabilities of snowfall for a given day through the entire winter, and for the amount of snow on a given day. These probabilities, however, are predicated on the absence of any long-range trends toward more severe or less severe winters. Indeed, most of us would testify that winters are not what they used to be. What trends do the long-range climatological records show? They show that, while it may be possible to plot short-term cyclic variations, there is no indication of a long-range trend toward either milder or colder winters.

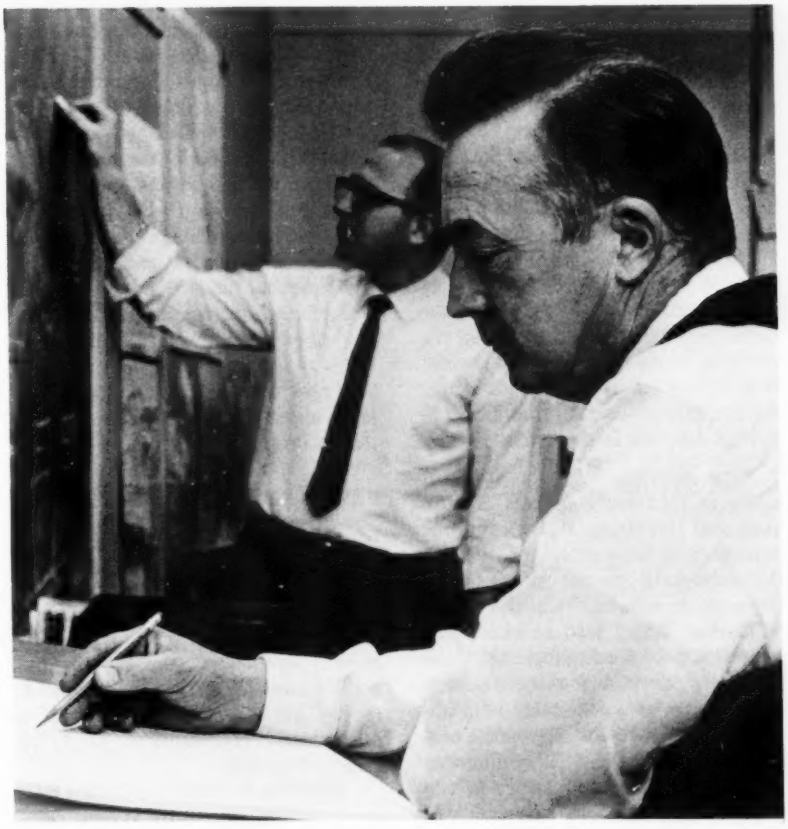

Mr. Salmela analyzes Boston snowfall data.

Mr. Henry A. Salmela is a research meteorologist with the Design Climatology Branch, Aerospace Instrumentation Laboratory, AFCRL. He is studying and analyzing the variability of winds in time and space and the errors in observing winds. He is also studying water vapor in the stratosphere and preparing a humidity atlas of the northern hemisphere. Mr. Salmela received his B.S. in Physics and Mathematics from the University of Massachusetts in 1939, and subsequently completed an Air Corps course in meteorology at the Massachusetts Institute of Technology in 1943. After World War II, he did graduate work in experimental statistics at North Carolina State College. Since joining the Air Force Cambridge Research Center, AFCRL's predecessor organization, in 1949, Mr. Salmela has taken courses in applied climatology and operations research at M.I.T. He is a member of the American Meteorological Society.

The Solid State as a Microwave Generator

JOSHUA H. ROSENBLOOM

Directorate of Engineering Sciences, AFOSR

INTRODUCTION

Within the last five years a large number of investigations have been devoted to the study of microwave energy from the solid state. The common feature of these studies is the generation of a traveling electromagnetic wave in the microwave frequency range when a static electric field above a threshold value is applied to a sample of a solid.

We concentrate on the microwave emission from the semiconductor indium antimonide (InSb) under the application of a magnetic field in the kilogauss range. This category has not as yet been assigned a designation in the literature. For ease in reference it will be denoted as the "InSb effect."

The motivation for this study of solids as microwave sources is both basic and technological. Basically, the phenomenon belongs to the field of the solid-state plasma, with special emphasis on instabilities in the plasma oscillations which lead to microwave propagation. Technologically, the solid-state plasma offers the possibilities of microwave generation with improved properties–the ruggedness and smaller size of the solid, millimeter and submillimeter frequencies arising from the higher natural frequencies of the solid-state plasma (of the order of 10^{12} Hertz).

HISTORY

The first observation of the InSb effect was made by Larrabee and Hicinbothem (1) of RCA Laboratories. They reported threshold electric and magnetic fields about 200 volts/cm and in the kilogauss (kg) range, respectively, to initiate the microwave emission. Threshold electric fields near 200 volts/cm suggested that an avalanche stage had been achieved forming an electron-hole plasma. Thus, it was postulated that holes were a necessary ingredient of the underlying mechanism. However, this conclusion was invalidated when Buchsbaum, Chynoweth, and Feldmann (2) of Bell Laboratories reported much lower threshold electric fields of about 10 volts/cm, well below the avalanche stage. The threshold magnetic fields remained in the kilogauss range. Since then, many notes (9-15) have been published in the literature extending the experimental data and attempting a theoretical understanding. Of the research efforts represented, AFOSR has supported the investigations of Ferry and Dougal (3) at the University of Texas and Bekefi and Bers (4) at MIT under the Joint Services Electronics Program.

EXPERIMENTAL ARRANGEMENTS

In typical experimental arrangements a sample of InSb was coupled to a wave guide either as an inductive post or by being mounted near a shorted coaxial transmission line. To prevent overheating the sample, the applied electric field was pulsed. A typical pulse was of the order of a microsecond repeatable 1 to 1,000 times per second.

Experiments were conducted over the following parameter ranges: temperature, 4.2°K (liquid helium) to 250°K, but mainly at 77°K (liquid nitrogen); frequency, 10 MHz to 102 GHz with most studies limited to a narrow frequency range; electric field, about 5 to 600 volts/cm; and magnetic field, 0.5 to 20 kg.

QUANTITATIVE RESULTS

The major characteristic of the InSb effect is that materials similar to InSb will emit microwaves of noise-like character and extremely broadband in frequency under the application of electric and magnetic fields above certain threshold levels provided the temperature is sufficiently low. It is agreed that significant parameters which affect the power output are the electric and magnetic fields, temperature, the frequency under consideration and the polarity of the electric field. (The effects of sample size are unclear.) The highest observed power output is of the order of a microwatt per MHz bandwidth.

The experimental data suggest several questions concerning the qualitative characteristics of possible theoretical modes: Can the InSb effect be considered a single phenomenon? There exists evidence of two distinct phenomena. The fact that the dependence of output power on electric field exhibits a sudden, vertical rise in the power output at the onset of the avalanche stage when the magnetic field is 8 kg points to two separate phenomena: above the avalanche stage the underlying mechanism requires an electron-hole plasma; below the avalanche stage the mechanism requires a pure electron plasma (Fig. 1). (2b) On the other hand, the other data continue smoothly through the avalanche transition, supporting the hypothesis of a single underlying mechanism.

Is the effect limited to InSb or does it have a wider, more fundamental base? The evidence points to the latter possibility. A number of semiconductors were investigated, but successful microwave emission was attained only with indium arsenide (InAs). (3a,b) The important point is that InSb and InAs have similar band-structure and transport properties, and that these properties differ significantly from those of the other semiconductors tried. In fact, InSb and InAs have the highest mobilities among the III-V indium and gallium compounds.

Is the effect a bulk phenomenon? The major evidence does imply a bulk phenomenon. A wide assortment of surface conditions were studied with the emission properties remaining unaltered. (2b,3a) However, some parameters change with a reversal of

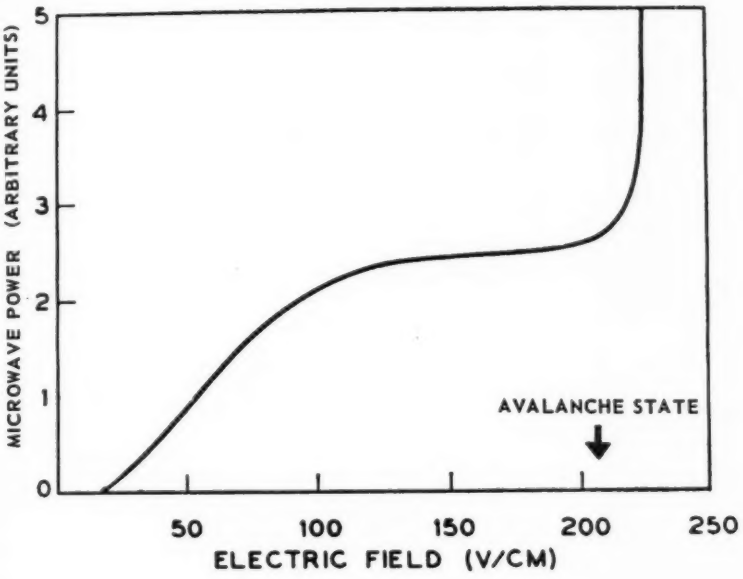

Figure 1. Power output vs. electric field. Note vertical rise at avalanche state. Magnetic field is 8kg and parallel to electric field. Frequency is 4.2 GHz. (Ref. 2b)

polarity. This may have surface implications. (2b,7 & 9)

Do the emission properties change with the orientation of magnetic and electric fields? The possible mechanisms to explain particular plasma phenomena are usually highly sensitive to such orientation. The answer depends on the range of electric fields being investigated. For very low fields, the power output decreases to zero as the orientation varies from 0° to 90°. (2a) At higher fields, the differences in power output were found to be insignificant. (3a, 6) However, a time delay develops between the output emission and the input electric field pulse at an orientation of 0°. This delay is absent at 90° (Figs. 2 and 3). (6)

POWER VARIATIONS

The quantitative goal is to determine the dependence of the power output on about a half dozen parameters. By fixing all the parameters but one, the dependence can be represented by a curve of power output vs. the one varying parameter. A certain cohesiveness of the data can be attained from a knowledge of the shapes or contours of the curves. For example, is the curve monotonic or more complex, with maxima and minima?

The topography of the curves of power output vs. magnetic field and temperature shows an especially rich structure. The interesting feature of the curve of power output vs. magnetic field is the maximum near 4 kg. (Fig. 4). (2b)

The dependence of power output on temperature suggests a maximum or a saturation effect. Maximum power occurs between 77° and 110°K, with the breadth of the maximum depending on the magnetic field (Fig. 5). (5) Similarly, whether the output at 4.2°K exceeds the power output at 77°K depends on the magnetic field. (4) In addition, at 4.2°K an unusual superposition of spikes, which is lacking at 77°K (4), will be observed on the curve of power output vs. magnetic field (Fig. 6). Amazingly, the spikes can be viewed as uniformly spaced along the magnetic-field coordinate (a spacing of 255 gauss for an electric field of 18 volts/cm). However, randomly, certain of the spikes are not excited.

There are other curves with the simpler monotonic structure–at least for ranges of parameters investigated thus far in any single investigator's experiments. Figure 7 is a composite

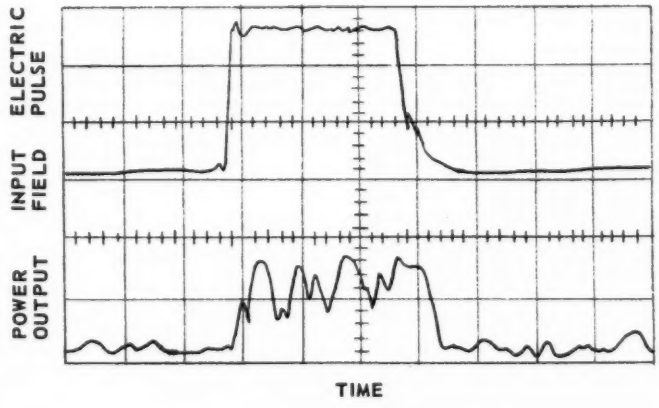

Figure 2. Comparison of power output and input electric field as a function of time. Note simultaneity of output and input. (Ref. 3a)

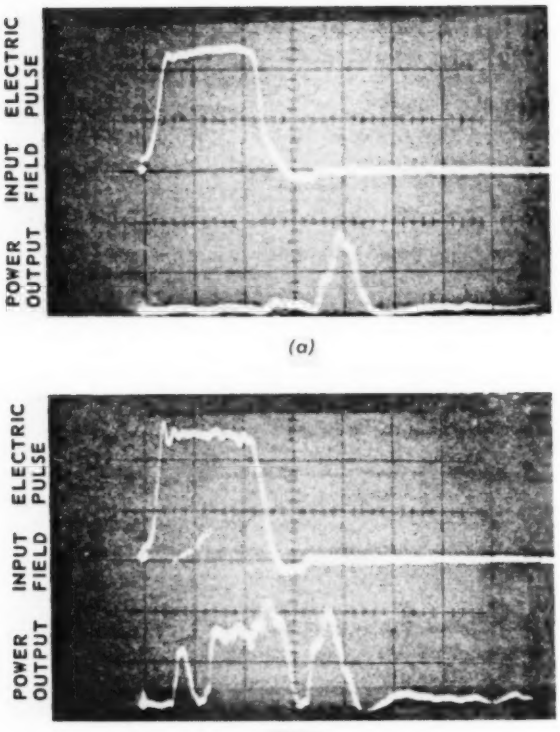

Figure 3. Comparison of power output and input electric field as a function of time. Note time delay of power output. Frequency = 10.2 GHz, electric field parallel to magnetic field. Electric field: (a) .50 volts/cm (near threshold); (b) 100 volts/cm. (Ref. 6)

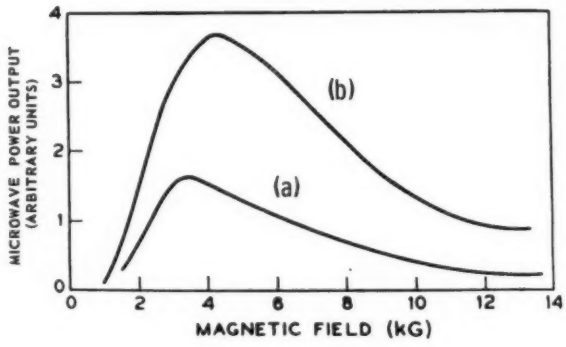

Figure 4. Power output vs. magnetic field. Note maxima. Frequency = 4.2 GHz. Electric field: (a) 25 volts/cm; (b) 38 volts/cm. (Ref. 2b)

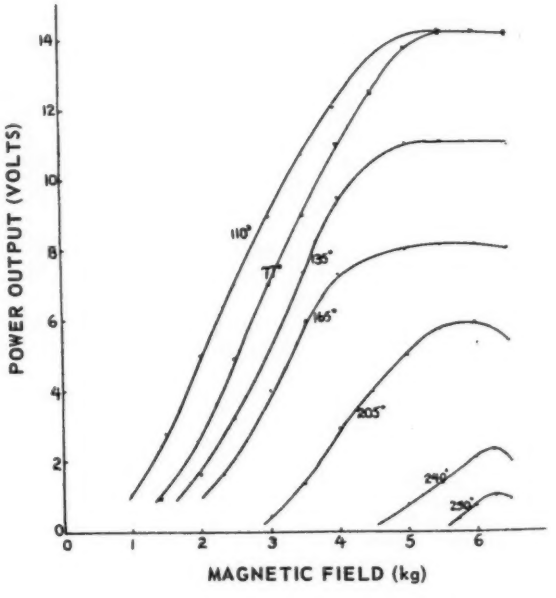

Figure 5. Power output vs. magnetic field and temperature. Note broad maxima between 77°K and 110°K as function of magnetic field. Electric field = 150 volts/cm. Frequency = 9.89 GHz. (Ref. 5)

group of threshold curves for a number of investigators relating the threshold values for the electric and magnetic fields to initiate the microwave emission. Figure 8 shows the decrease of power output with increase of frequency.

EXPERIMENTAL ACCURACY

A presentation of experimental results should include an assessment of their accuracy. In general, the experimental probing of the InSb effect is still in its early stages so that judicious care must be exercised in attributing absolute significance to the data.

It is difficult to compare the conclusions of different investigators. Rarely are experiments performed under the same conditions. Vagaries due to experimental arrangements have still to be separated out from properties characteristic of the phenomenon. Even for the same investigator different samples show wide differences. Dispersions of 20% and 10db in power outputs measured under the same conditions for different samples have been reported. (3a, 4) In fact, samples of InSb have been discovered whose threshold magnetic field is zero. (3d)

THEORY

The basic approach is to consider the system of charged particles of a semiconductor (electrons, ions, and possibly holes) as a plasma. Due to the long-range action of the coulomb forces, the charged particles act collectively to sustain certain specific modes of oscillations within themselves and in associated electromagnetic fields.

The application of an external

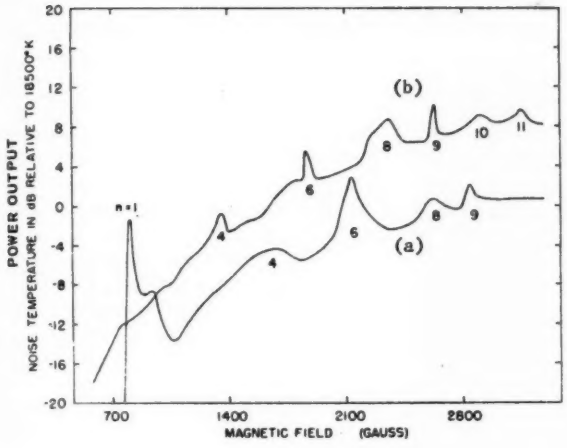

Figure 6. Power output vs. magnetic field. Note uniformly spaced spikes randomly excited. Integers indicate sequence order of spikes. Temperature = 4.2°K. Frequency = 3GHz. Electric field: (a) 10 volts/cm; (b) 18 volts/cm. (Ref. 4)

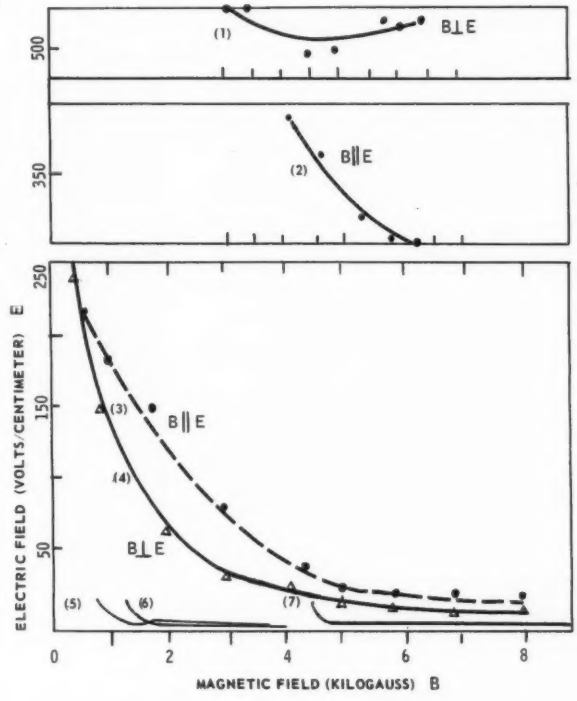

Figure 7. Threshold curves for initiating microwave emission.

(1,2) 77°K, 15 GHz (Ref. 1)
(3,4) 77°K, 8.4 GHz (Ref. 3a)
(5) 77°K, 3.0 GHz (Ref. 4)
(6) 4.2°K, 3.0 GHz (Ref. 4)
(7) 77°K, 2-4 GHz (Ref. 7)

electric field introduces a streaming in the charged particles. If this streaming attains certain characteristic features, an instability ensues in one of the plasma modes. That is, the particles give up their energy to this mode so that the latter grows into a propagating electromagnetic wave along the semiconductor sample.

Thus, the problem becomes one of identifying the features of the streaming charged particles which initiate instabilities and the particular plasma mode excited to cause the radiation. No consistent answer has been developed as yet. Furthermore, the impreciseness of the experimental picture has supported a variety of theoretical approaches including two-stream instability, (12) traveling helicon wave, (13, 14) phonon interaction, (15) and impurity effects. (3a)

SUMMARY

One major conclusion stands out. The InSb effect has a rich structure. The power output depends upon about a half dozen variables. A curve relating power output to one of these variables will often involve complex interactions* rather than simple linear

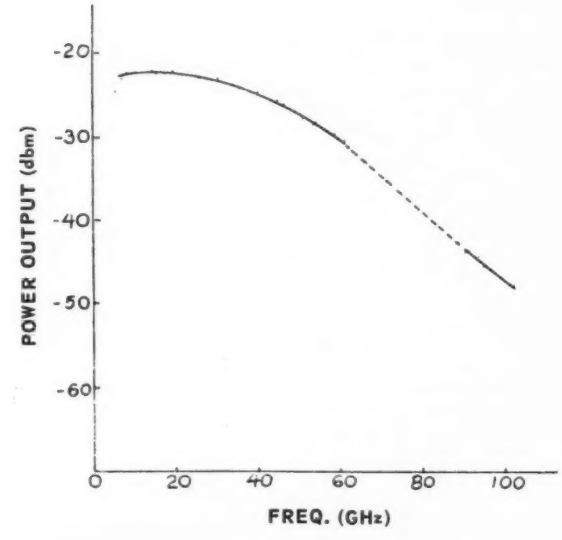

Figure 8. Power output vs. frequency. Electric field = 200 volts/cm. Transverse magnetic field = 5.6 kg. (Ref. 6)

**For example, Ancker-Johnson (8) has found a set of conditions for microwave emissions from InSb of the p-type with no magnetic field required.*

relationships. Qualitative generalizations in one range of the variables cannot reliably be extended to other ranges.

Experimental probing is still in its early stages, and no consistent theoretical model of the phenomenon has as yet been developed. Technological exploitation is dependent upon a better understanding of this phenomenon. The number of unusual interrelationships of the variables suggests a potential for application.

REFERENCES

(1) *Larrabee, R. D. and W. A. Hicinbothem, paper presented at National Conference on Physics of Semiconductors, Paris, 1964; included in Plasma Effects in Solids, Paris: Dunod, 1965, p. 181.*

(2) *Buchsbaum, S. J., A. G. Chynoweth and W. L. Feldmann–a) Appl. Phys. Letters, 6, 67, 1965; b) J. Appl. Phys., 37, 2922, 1966.*

(3) *Ferry, D. K. and A. A. Dougal–a) "Microwave Emission from Bulk Semiconductors," Tech. Report No. 16, Laboratories of Electronics and Related Science Research, University of Texas, May 1966; b) Appl. Phys. Letters, 7, 318, 1965; c) J. Appl. Phys., 36, 3684, 1965; d) Zeitschrift für Naturf., 22a, 576, 1967.*

(4) *Bekefi, G. and A. Bers–a) Quarterly Progress Report No. 85, Research Laboratory of Electronics, Massachusetts Institute of Technology, April 1967, pp. 128-134; b) Phys. Rev. Letters, 19, 24, 1967.*

(5) *Poehler, T. O., Appl. Phys. Letters, 10, 356, 1967.*

(6) *Poehler, T. O., J. R. Apel and A. K. Hochberg, Appl. Phys. Letters, 10, 244, 1967.*

(7) *Musha, T., F. Lundvall and J. Hägglund, Appl. Phys. Letters, 8, 157, 1966.*

(8) *Ancker-Johnson, B., Appl. Phys. Letters, 10, 279, 1967.*

(9) *Eidson, J. C. and G. S. Kino, Appl. Phys. Letters, 8, 183, 1966.*

(10) *Suzuki, K., J. Appl. Phys. (Japan), 4, 42, 1965.*

(11) *Morisaki, H. and Y. Iniushi, J. Appl. Phys. (Japan), 5, 343, 1966.*

(12) *Vural, B. and M.C. Steele, Phys. Rev., 139A, A300, 1965.*

(13) *Steele, M. C., see Ref. 1, p. 189.*

(14) *Bok, J. and P. Nozierres, Jour. Phys. Chem. Solids, 24, 709, 1963.*

(15) *Musha, T. and A. Bers, Quarterly Progress Report No. 79, Research Laboratory of Electronics, Massachusetts Institute of Technology, October 1965, p. 99.*

error bounds for the numerical solution of a linear system of ordinary differential equations

DR. CHARLES KELLER
and
DR. KARL G. GUDERLEY

Applied Mathematics Research Laboratory, ARL

Considerable efforts have been made in the past to devise schemes for the numerical integration of systems of ordinary differential equations. Judging from examples of the results, these efforts have succeeded. For nearly all applications the schemes that resulted can be considered extremely satisfactory.

Yet, in spite of their undisputed successes, these methods do not convey a clear idea of the error in the solution. Instead, they state that the magnitude of the error behaves like some power of the length of the integration step and require that the length of the integration step be reduced, if necessary, so as to achieve some prescribed accuracy for an individual step. Thus, some mathematicians are inclined to exclude the use of differential equations as a tool for problems where exact statements on error bounds are desirable.

Of course, there exist rigorous methods for bounding the errors that are encountered in the solution of a system of ordinary differential equations; but frequently these bounds are so wide that they should be considered useless. In the present article we sketch a geometrical interpretation of the task of bounding the errors.

Some of the underlying ideas for this work were obtained by Dr. Guderley in the work reported in the

Blanch Anniversary volume entitled *On Error Bounds For the Solution of Systems of Ordinary Differential Equations* by Dr. Guderley and Marian Valentine (Ref. 1). The present form of these ideas, as given below, was developed by Dr. Guderley and Dr. Keller. A procedure for the computation of error bounds is being programmed by Mr. M. C. Breiter.

The initial value problem for a linear system of ordinary differential equations in vector notation is

$$(1)\quad \begin{aligned} Y'(x) &= A(x)\,Y(x) + F(x), \quad a \le x \le b \\ Y(a) &= Y_o. \end{aligned}$$

In the first equation (1) Y(x) and F(x) denote n-dimensional vectors and A(x) a square matrix of order n. The components $F_i(x)$ of F(x) and the entries $a_{ij}(x)$ of A(x) are continuous functions of the independent variable x for x in some open interval containing the interval [a, b].

Under the conditions assumed on A(x) and F(x) there is, for each value x_o in [a, b] and each point (x_o, Y_o) in (n + 1)-space, a unique vector function Y(x) which satisfies the differential equation (1) such that $(x_o, Y(x_o)) = (x_o, Y_o)$. The uniqueness condition implies continuity with respect to the initial values Y_o.

We assume the numerical solution has been determined in a stepwise fashion. That is, the interval [a, b] has been divided into subintervals and, for each subinterval, some expression has been determined as an approximation to the desired solution Y(x).

Let $x_i \le x \le x_f$ denote one of these subintervals and Z(x) the approximation to Y(x) on this interval. It is assumed that Z(x) can be evaluated for each value of x, $x_i \le x \le x_f$, by some small number of operations. Now Z(x) satisfies the system of differential equations

$$(2)\quad \begin{aligned} Z'(x) &= A(x)\,Z(x) + G(x), \quad x_i \le x \le x_f \\ Z(x_i) &= Z_i, \end{aligned}$$

where G(x) = Z' (x) - A(x)Z(x).

Throughout the interval $x_i \le x \le x_f$ the *error* is y(x) = Y(x) - Z(x). The equation for the error y(x) is obtained by subtracting equation (2) from equation (1). This gives

$$(3)\quad \begin{aligned} y'(x) &= A(x)y(x) + r(x), \quad x_i \le x \le x_f \\ y(x_i) &= Y(x_i) - Z(x_i), \end{aligned}$$

where r(x) = F(x) - G(x).

For a given x the error is a vector. One should distinguish clearly between the error and an error bound. An error bound describes a set of vectors one of which should be the error vector.

We consider three factors which contribute to the error bound and call these factors the initial error, the truncation error, and the rounding error.

If x_i is different from a, then $y(x_i)$ in the second of equations (3) is not known; but we may suppose that a bound for $y(x_i)$ has been determined. Each vector y_o which is characterized by this bound for $y(x_i)$ is a possible set of initial conditions for equation (3). Thus for each vector y_o determined by the bound for $y(x_i)$ there is a solution of equation (3) which is equal to y_o initially. One of these solutions should be the error. We call the totality of such solutions the *error tube.*

If each vector function in this totality of solutions is evaluated at the same arbitrary but fixed value of x, then a set of vectors is obtained, one of which is the error for this x. The set of vectors so obtained we call the *error figure.* Since one of the vectors in the error figure is the error vector, the set of vectors determined by an error bound must include the error figure. The error figure is determined by the *initial error* figure (the bound on $y(x_i)$) and the differential equation (3).

If Z(x) is substituted into the original differential equation (1) we obtain

$$(4)\quad r(x) = A(x)Z(x) + F(x) - Z'(x).$$

The vector valued function r(x) is called the *residual.* It represents the amount by which the approximate solution Z(x) fails to satisfy the original system of equations. We refer to the contributions of the residual to the error as the *truncation error.* Lastly, the contribution to the error resulting from limitations in the precision with which arithmetic operations are performed we call *rounding error.* Thus the error bound must account for the propagation of the initial error through the interval and the additional errors introduced by the residual and rounding. The rounding error may be taken into account by expanding the error tube.

The error tube is a point set in (n + 1)-space. The boundary of this error tube constitutes an n-surface S. This n-surface "bounds" the error vector. It is clear that, under the conditions accepted above, this n-surface is the *best* possible bound for the error vector. Now any other surface which contains S also bounds the error vector. One might note that the determination of a surface which encloses the error tube is closely related to the determination of a Lyapunov function.

The error figure (the cross section of the error tube in a hyperplane x=constant) can be rather complicated and may change considerably with x. We try to determine, by means of differential inequalities, a surface B that includes the error tube. In general, it is not possible to determine B so that it represents the error figure exactly.

Almost all methods for specifying error bounds determine a surface B such that its trace in a hyperplane perpendicular to the x-axis is either an n-circle (2 norm) or an n-square (infinity norm). With such a representation one can obtain rigorous error bounds; there are examples where these error bounds are good. However, there are also examples where such bounds exhibit an excessive growth rate, that is, the error bounds are overly pessimistic.

Analyzing these examples, one finds that an excessive rate of growth of the error bound occurs whenever the error figure undergoes periodic changes of its form and the characterization chosen is unable to follow these changes. This excessive growth occurs even if truncation and rounding errors are neglected. One concludes, therefore, that the undesired growth

of the error bound occurs if the error figure is not properly characterized.

It is not too difficult to show that, if the initial error figure is an n-ellipsoid and if rounding error is neglected, then the error figure is an n-ellipsoid throughout the interval $x_i \leq x \leq x_f$. Thus, in order to keep the rate of growth of the error bound from becoming excessively large too soon, we determine the surface B so that its cross section is ellipsoidal and we strive to do this in such a way as to be a good characterization of the error figure.

It is fortunate that, with the characterization of the error bound as dictated by the problem itself, it is easy to give a bound on the error in a conventional fashion, that is, as a bound on the components of the error.

A short written communication (Ref. 2) from W. Kahn of the University of Toronto seemingly indicates that he is investigating a procedure similar to the one proposed above. Other proposals for determining error bounds are given in Refs. 3, 4, and 5. The last two appear to suffer from the defect that motivated this investigation, namely, the bounds become excessively large.

REFERENCES

(1) Guderley, Karl G. and Marian Valentine, On Error Bounds for the Solution of Systems of Ordinary Differential Equations, Blanch Anniversary Volume, Aerospace Research Laboratories, Office of Aerospace Research, United States Air Force, February 1967.

(2) Kahn, W., private communication, University of Toronto, Canada, 1967.

(3) Krückeberg, F. and H. Unger, "On the Numerical Integration of Ordinary Differential Equations and the Determination of Error Bounds, Symposium Provisional Computation Center, Basel: Birkhauser Verlag, 1960.

(4) Moore, Ramon E., Interval Analyses, Englewood Cliffs, N.J.: Prentice-Hall, 1966.

(5) Schroeder, Johann, "Fehlerabschaetzungen mit Rechenanlagen bei gewoehnlichen Differentialgleichungen erster Ordnung," Numerische Mathematik, 3, 1961, pp. 39-61.

From the Editor:

With this issue of the OAR Research Review, we have taken another step forward in our continuing effort to make this publication more readable. We hope the modified format accomplishes this purpose. Please write your comments, if any, to: Hq OAR (RRYC), 1400 Wilson Blvd., Arlington, Va., 22209.

GPO 939-676